Charged pion form factor between $Q^2 = 0.60$ and 2.45 GeV^2. II. Determination of, and results for, the pion form factor

G.M. Huber,[1] H.P. Blok,[2,3] T. Horn,[4,5] E.J. Beise,[4] D. Gaskell,[5] D.J. Mack,[5] V. Tadevosyan,[6] J. Volmer,[2,7] D. Abbott,[5] K. Aniol,[8] H. Anklin,[9,5] C. Armstrong,[10] J. Arrington,[11] K. Assamagan,[12] S. Avery,[12] O.K. Baker,[12,5] B. Barrett,[13] C. Bochna,[14] W. Boeglin,[9] E.J. Brash,[1] H. Breuer,[4] C.C. Chang,[4] N. Chant,[4] M.E. Christy,[12] J. Dunne,[5] T. Eden,[5,15] R. Ent,[5] H. Fenker,[5] E.F. Gibson,[16] R. Gilman,[17,5] K. Gustafsson,[4] W. Hinton,[12] R.J. Holt,[11] H. Jackson,[11] S. Jin,[18] M.K. Jones,[10] C.E. Keppel,[12,5] P.H. Kim,[18] W. Kim,[18] P.M. King,[4] A. Klein,[19] D. Koltenuk,[20] V. Kovaltchouk,[1] M. Liang,[5] J. Liu,[4] G.J. Lolos,[1] A. Lung,[5] D.J. Margaziotis,[8] P. Markowitz,[9] A. Matsumura,[21] D. McKee,[22] D. Meekins,[5] J. Mitchell,[5] T. Miyoshi,[21] H. Mkrtchyan,[6] B. Mueller,[11] G. Niculescu,[23] I. Niculescu,[23] Y. Okayasu,[21] L. Pentchev,[10] C. Perdrisat,[10] D. Pitz,[24] D. Potterveld,[11] V. Punjabi,[15] L.M. Qin,[19] P.E. Reimer,[11] J. Reinhold,[9] J. Roche,[5] P.G. Roos,[4] A. Sarty,[13] I.K. Shin,[18] G.R. Smith,[5] S. Stepanyan,[6] L.G. Tang,[12,5] V. Tvaskis,[2,3] R.L.J. van der Meer,[1] K. Vansyoc,[19] D. Van Westrum,[25] S. Vidakovic,[1] W. Vulcan,[5] G. Warren,[5] S.A. Wood,[5] C. Xu,[1] C. Yan,[5] W.-X. Zhao,[26] X. Zheng,[11] and B. Zihlmann[27,5]

(The Jefferson Lab F_π Collaboration)

[1] *University of Regina, Regina, Saskatchewan S4S 0A2, Canada*
[2] *VU university, NL-1081 HV Amsterdam, The Netherlands*
[3] *NIKHEF, Postbus 41882, NL-1009 DB Amsterdam, The Netherlands*
[4] *University of Maryland, College Park, Maryland 20742*
[5] *Physics Division, TJNAF, Newport News, Virginia 23606*
[6] *Yerevan Physics Institute, 375036 Yerevan, Armenia*
[7] *DESY, Hamburg, Germany*
[8] *California State University Los Angeles, Los Angeles, California 90032*
[9] *Florida International University, Miami, Florida 33119*
[10] *College of William and Mary, Williamsburg, Virginia 23187*
[11] *Physics Division, Argonne National Laboratory, Argonne, Illinois 60439*
[12] *Hampton University, Hampton, Virginia 23668*
[13] *Saint Mary's University, Halifax, Nova Scotia, Canada*
[14] *University of Illinois, Champaign, Illinois 61801*
[15] *Norfolk State University, Norfolk, Virginia*
[16] *California State University, Sacramento, California 95819*
[17] *Rutgers University, Piscataway, New Jersey 08855*
[18] *Kyungpook National University, Taegu, Korea*
[19] *Old Dominion University, Norfolk, Virginia 23529*
[20] *University of Pennsylvania, Philadelphia, Pennsylvania 19104*
[21] *Tohoku University, Sendai, Japan*
[22] *New Mexico State University, Las Cruces, New Mexico 88003-8001*
[23] *James Madison University, Harrisonburg, Virginia 22807*
[24] *DAPNIA/SPhN, CEA/Saclay, F-91191 Gif-sur-Yvette, France*
[25] *University of Colorado, Boulder, Colorado 76543*
[26] *M.I.T.–Laboratory for Nuclear Sciences and Department of Physics, Cambridge, Massachusetts 02139*
[27] *University of Virginia, Charlottesville, Virginia 22901*

(Dated: September 18, 2008)

The charged pion form factor, $F_\pi(Q^2)$, is an important quantity which can be used to advance our knowledge of hadronic structure. However, the extraction of F_π from data requires a model of the ^{1}H$(e,e'\pi^+)n$ reaction, and thus is inherently model dependent. Therefore, a detailed description of the extraction of the charged pion form factor from electroproduction data obtained recently at Jefferson Lab is presented, with particular focus given to the dominant uncertainties in this procedure. Results for F_π are presented for Q^2=0.60-2.45 GeV^2. Above $Q^2 = 1.5$ GeV^2, the F_π values are systematically below the monopole parameterization that describes the low Q^2 data used to determine the pion charge radius. The pion form factor can be calculated in a wide variety of theoretical approaches, and the experimental results are compared to a number of calculations. This comparison is helpful in understanding the role of soft versus hard contributions to hadronic structure in the intermediate Q^2 regime.

PACS numbers: 14.40.Aq,13.40.Gp,13.60.Le,25.30.Rw,11.55.Jy

I. INTRODUCTION

There is much interest in trying to understand the structure of hadrons, both mesons and baryons, in terms of their constituents, the quarks and gluons. However, this structure is too complicated to be calculated rig-

orously in Quantum Chromodynamics (QCD) because perturbative QCD (pQCD) methods are not applicable in the confinement regime. Chiral Perturbation Theory can give valuable insights, but it is limited to small values of the photon virtuality Q^2. Hence, in the intermediate Q^2 regime one has to resort to models like the constituent quark model or methods employing Light-Cone (LC) dynamics or the Bethe-Salpeter (plus Dyson-Schwinger) equation, or to other approaches such as the use of dispersion relations or (QCD or LC) sum rules.

Transitions and (transition) form factors are crucial elements for gauging the ideas underlying these QCD-based models. For example, the constituent quark model gives a fairly good description of the meson and baryon spectrum and some transitions, but quark effective form factors are typically required when describing hadronic form factors in the experimentally accessible Q^2 region. In this framework, the study of hadronic form factors can thus be viewed as a study of the transition from constituent to current quark degrees of freedom. As exemplified by the many calculations of it, the electric form factor of the pion, F_π, is one of the best observables for the investigation of the transition of QCD effective degrees of freedom in the soft regime, governed by all kinds of quark-gluon correlations at low Q^2, to the perturbative (including next-to-leading order and transverse corrections) regime at higher Q^2.

In contrast to the nucleon, the asymptotic normalization of the pion wave function is known from pion decay. The hard part of the π^+ form factor can be calculated within the framework of pQCD as the sum of logarithms and powers of Q^2 [1]

$$F_\pi(Q^2) = \frac{4\pi C_F \alpha_s(Q^2)}{Q^2}\left|\Sigma_{n=0}^{\infty} a_n \left(log(\frac{Q^2}{\Lambda^2})\right)^{-\gamma_n}\right|^2 [1 + O(\alpha_s(Q^2), m/Q^2)], \quad (1)$$

which in the $Q^2 \to \infty$ limit becomes [1, 2]

$$F_\pi(Q^2) \xrightarrow[Q^2\to\infty]{} \frac{16\pi\alpha_s(Q^2) f_\pi^2}{Q^2}, \quad (2)$$

where $f_\pi = 93$ MeV is the pion decay constant [3].

Because the pion's $\bar{q}q$ valence structure is relatively simple, the transition from "soft" (non-perturbative) to "hard" (perturbative) QCD is expected to occur at significantly lower values of Q^2 for F_π than for the nucleon form factors [4]. Some estimates [5] suggest that pQCD contributions to the pion form factor are already significant at $Q^2 \geq 5$ GeV^2. On the other hand, a recent analysis [6] indicates that non-perturbative contributions dominate the pion form factor up to relatively large values of Q^2, giving more than half of the pion form factor up to Q^2=20 GeV^2. Thus, there is an ongoing theoretical debate on the interplay of these hard and soft components at intermediate Q^2, and high quality experimental data are needed to help guide this discussion.

In this work, we concentrate exclusively on the spacelike region of the pion form factor. For recent measurements in the timelike region see Ref. [7]. At low values of Q^2, where it is governed by the charge radius of the pion, F_π has been determined up to Q^2=0.253 GeV^2 [8, 9] from the scattering of high-energy pions by atomic electrons. For the determination of the pion form factor at higher values of Q^2, one has to use high-energy electroproduction of pions on a nucleon, i.e., employ the ^{1}H$(e, e'\pi^+)n$ reaction. For selected kinematic conditions, the longitudinal cross section is very sensitive to the pion form factor. In this way, data for F_π have been obtained for values of Q^2 up to 10 GeV^2 at Cornell [10, 11, 12]. However, those data suffer from relatively large statistical and systematic uncertainties. More precise data were obtained at the Deutsches Elektronen-Synchrotron (DESY) [13, 14]. With the availability of high-intensity electron beams, combined with accurate magnetic spectrometers at the Thomas Jefferson National Accelerator Facility (JLab), it has been possible to determine L/T separated cross sections with high precision. The measurement of these cross sections in the regime of Q^2=0.60-1.60 GeV^2 [Experiment Fpi-1 [15, 16]] and Q^2=1.60-2.45 GeV^2 [Experiment Fpi-2 [17]] are described in detail in the preceding paper [18]. In this paper, it is discussed how to determine F_π from measured longitudinal cross sections, the values determined from the JLab and DESY data are presented, and the results of various theoretical calculations are compared with the experimental data.

Since the pion in the proton is virtual (off its mass-shell), the extraction of F_π from the measured electroproduction cross sections requires some model or procedure. In the next section, the methods that have been used to determine F_π from the data are discussed. Section III presents the adopted extraction method and the values of F_π thus determined, including a full discussion of the uncertainties resulting from the experimental data and those from the adopted extraction procedure. Various model calculations of F_π are discussed and compared to the data in section IV. In the final section, some conclusions are drawn and an outlook for the future is given.

II. METHODS OF DETERMINING THE PION CHARGE FORM FACTOR FROM DATA

The measurement of the pion form factor is challenging. As stated in the introduction, at low Q^2 F_π can be measured in a model-independent manner via the elastic scattering of π^+ from atomic electrons, such as has been done up to Q^2=0.253 GeV^2 at Fermilab [8] and at the CERN SPS [9]. It is not possible to access significantly higher values of Q^2 with this technique because of limitations in the energy of the pion beam together with the unfavorable momentum transfer. Therefore, at higher values of Q^2 F_π must be determined from pion electroproduction on the proton. The dependence on F_π enters the cross section via the t-channel process, in which the incident electron scatters from a virtual pion, bringing it on-shell. This process dominates near the pion-pole at $t = m_\pi^2$, where t is the Mandelstam variable. The physical region for t in pion electroproduction is negative, so measurements should be performed at the smallest attainable values of $-t$. To minimize background contributions, it is also necessary to separate out the longitudinal cross section $\sigma_{\rm L}$, via a Rosenbluth L/T(/LT/TT) separation [19].

The minimum physical value of $-t$, $-t_{min}$, is non-zero and increases with increasing Q^2 and decreasing value of the invariant mass, W, of the produced pion-nucleon system. Carlson and Milana [20] have estimated an approximate upper limit for the value of $-t_{min}$ of the data appropriate for the extraction of the pion form factor by studying the competing non-pole QCD processes, which may complicate the extraction of F_π at higher Q^2. They found that the background ratio M_{pQCD}/M_{pole} rises dramatically once $-t_{min} > 0.20$ GeV^2. Their concern stemmed from the large value of $-t$ in some of the Cornell results, which have $-t_{min} > 0.4$ GeV^2 [12]. Therefore, reliable F_π measurements should be performed at smaller $-t$ and thus higher W (for a fixed Q^2). The results presented in this paper respect this $-t_{min} < 0.20$ GeV^2 upper limit. It is yet to be determined if reliable F_π measurements can be made in the future at larger $-t$.

The value of $F_\pi(Q^2)$ can then be determined from the data by trying to extrapolate the measured longitudinal cross sections at small values of $-t$ to the pole at $t = m_\pi^2 = 0.02$ GeV^2, or by comparing the measured longitudinal cross section at small values of $-t$ to the best available model for the ^{1}H$(e, e'\pi^+)n$ reaction, adjusting the value of F_π in the latter. The presence of the nucleon and its structure complicates the theoretical model used, and so an unavoidable implication of this method is that the extracted pion form factor values are model dependent. The differential cross sections $\sigma_{\rm L}$ versus t over some range of Q^2 and W are the actual observables measured by the experiment. It is important to note that in all cases the use of a model to extract F_π is justified only if the model correctly predicts the t-dependence and magnitude of the $\sigma_{\rm L}$ data as well as the dependence on the invariant mass W of the photon-nucleon system.

A. Chew-Low Extrapolation Method

Frazer [21] originally proposed that F_π be extracted from $\sigma_{\rm L}$ via a kinematic extrapolation to the pion-pole, and that this be done in an analytical manner using the so called Chew-Low extrapolation [22]. The used Born formula is not gauge invariant [23], but in principle should give F_π, nonetheless, when extrapolating to the pole.

The last serious attempt to extract the space-like pion form factor from electroproduction data via the Chew-Low method was by Devenish and Lyth [24] in 1972. Most of the data used were unseparated cross sections. The extrapolation failed to produce a reliable result, because different polynomial fits that were equally likely in the physical region gave divergent values of the form factor when extrapolated to the pion-pole at $t = m_\pi^2$. Since then, the quality of the π^+ electroproduction dataset has improved immensely, and separated longitudinal cross sections can now be used, avoiding the complications stemming from the other parts of the cross section. Therefore, it has been suggested to us that it may be appropriate to revisit the Chew-Low extrapolation method.

However, before trying this method on the new data, it should be tested to see how reliably one can extrapolate to the pole. We start with high precision $\sigma_{\rm L}$ 'pseudo-data' generated as a function of $-t$ with the VGL Regge model. This model gives a fair to good description of a wide body of pion photo- and electroproduction data (see section II C). The kinematic conditions for the test are $Q^2 = 1.594$ GeV^2 and $W = 2.213$ GeV, similar to our Fpi-2 data. The input value of the pion form factor in the model was $F_\pi = 0.244$. The model $\sigma_{\rm L}$ cross sections were then used in a Chew-Low type extrapolation, with the challenge being to see if the Chew-Low extrapolation is able to reproduce (within fitting uncertainties) the input F_π-value.

The basis of the Chew-Low method is the Born-term model (BTM) formula for the pion-pole contribution to $\sigma_{\rm L}$. We use the BTM of Actor, Korner and Bender [25], where pion-pole contribution to $\sigma_{\rm L}$ is given by

$$N\frac{d\sigma_L}{dt} = 4\hbar c\ (eg_{\pi NN})^2\ \frac{-t}{(t-m_\pi^2)^2}\ Q^2F_\pi^2(Q^2), \qquad (3)$$

where $e^2/(4\pi\hbar c) = 1/137$ and N, which depends on the flux factor used in the definition of $\frac{d\sigma_L}{dt}$, is given in our case by

$$N = 32\pi(W^2-m_p^2)\sqrt{(W^2-m_p^2)^2+Q^4+2Q^2(W^2+m_p^2)} \qquad (4)$$

[26, 27]. A monopole parameterization of the $g_{\pi NN}$ form factor is typically used to determine its value at t-values away from the pion-pole

$$g_{\pi NN}(t) = g_{\pi NN}(m_\pi^2)\Big(\frac{\Lambda_\pi^2-m_\pi^2}{\Lambda_\pi^2-t}\Big), \qquad (5)$$

where $g_{\pi NN}(m_\pi^2)$ is the experimental value of 13.4 [28]. This is also the value used in the VGL calculations. We

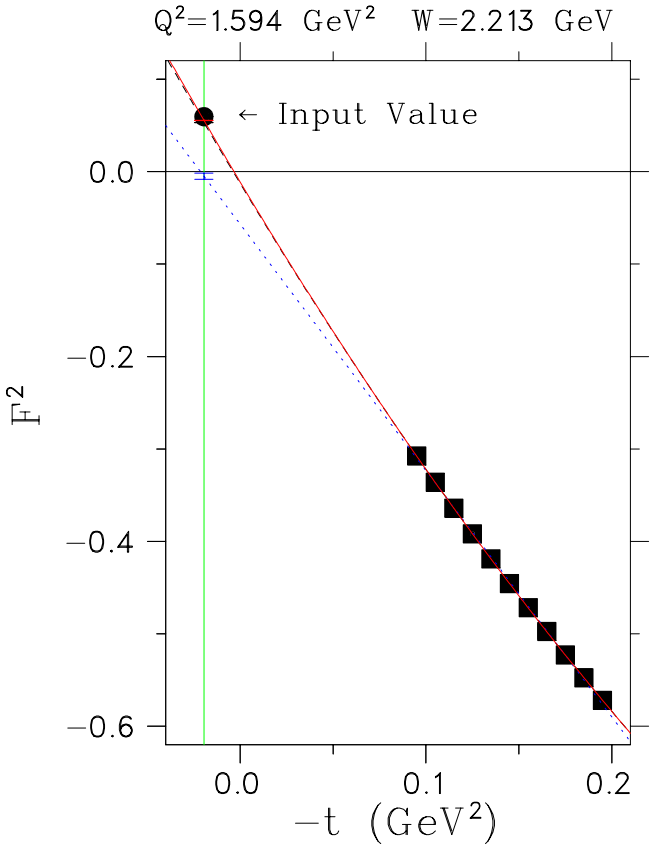

FIG. 1: (Color online) Linear (dotted), quadratic (dashed) and cubic (solid line) extrapolations of F^2 to the pole as computed from Eqn. 6. The boxes are a VGL Regge model calculation for $\sigma_{\rm L}$ at fixed $W = 2.213$ GeV and $Q^2 = 1.594$ GeV^2, calculated with F_π=0.244. The lower limit of the box range is the kinematic endpoint of these Q^2, W values, while the upper limit is given by the t-range of our experiment. The input F_π value in the model is indicated by the bullet placed at the pion-pole.

use the $\Lambda_\pi = 0.80$ GeV result from the QCD Sum Rules calculation by T. Meissner [29], but because of the extrapolation to the pole the final result does not depend significantly upon the value chosen.

For the Chew-Low extrapolation, one plots the value of

$$F^2 = \frac{N}{4\hbar c\,(eg_{\pi NN})^2}\frac{(t-m_\pi^2)^2}{-Q^2 m_\pi^2}\frac{d\sigma_L}{dt} \qquad (6)$$

versus $-t$, which for a pure pole cross section gives a straight line passing through the origin, with value $F_\pi(Q^2)$ at the pole ($t = m_\pi^2$). Other contributions to the cross section, which have to be present, because the pole contribution alone is not gauge invariant, will change this behavior, but since they do not contain the $\frac{1}{(t-m_\pi^2)^2}$ factor, they will not influence the value of F^2 at the pole. However, it is not a priori given that the behavior as function of $-t$ is linear, quadratic, or of higher order, thus introducing a 'model' (extrapolation) uncertainty.

Values of F^2 for the generated pseudodata, together with linear, quadratic and cubic extrapolations to the pole are shown in Fig. 1. Also shown is the input form factor value in the VGL model, plotted at the pion-pole. Quadratic and higher-order extrapolations are almost indistinguishable and give a very good description of the (pseudo)data, but miss the input value of F_π. This was true for all cases that were investigated, from $Q^2 = 0.60$ to 2.45 GeV^2, the deviation from the input F_π-value being 6-15%, depending on the case and the order of the extrapolation polynomial. Overall, there was no consistent trend for the order of polynomial which was best able to reproduce the input form factor value.

This study indicates that even if $\sigma_{\rm L}$ is very well known over a range of physically-accessible t, the Chew Low extrapolation yields inconsistent results. The extrapolated result depends greatly upon the choice of quadratic cubic, or higher-order function, which all give a very good description of the data in the physical region. This indicates that the t-dependence of data in the physical region is insufficient to uniquely constrain the extrapolation through the unphysical region to the pole, even if the data have small relative uncertainties. Furthermore, even though modern data such as the JLab $\sigma_{\rm L}$ data are much more precise than those previously available, they still comprise 4-6 t-bins only, each with statistical and systematic uncertainties of 5-10%. Therefore, any polynomial extrapolation of such data to the pole will be more unreliable than the pseudodata test case shown here. Therefore, the Chew-Low extrapolation technique cannot be used to reliably determine the pion form factor from a realistic $\sigma_{\rm L}$ data set.

B. Early Extractions of F_π

Brown *et al.* [30] at CEA were the first to embrace the use of theoretical input to determine F_π from their data. They used the model of Berends [31], which includes the dominant isovector Born term, with corrections for t values away from the pole by means of fixed-t dispersion relations. This model was also used by Bebek *et al.* for the analysis of the first two sets of Cornell data [10, 11]. The model gave a fair description of the data, but systematically underpredicted the LT term of the cross section and the t-dependence of the data.

Until then, data were obtained at one (larger) value of the photon polarization parameter ϵ only. In the third Cornell experiment [12], data were taken at low values of ϵ, so that in combination with the earlier data an L/T separation could be performed at Q^2-values of 1.19, 2.00 and 3.32 GeV^2. The value of $\sigma_{\rm T}$ was found to be substantially larger than predicted by Berends, especially at larger Q^2. The values obtained for $\sigma_{\rm L}$ had such large error bars that they were not used to determine F_π. Instead, use was made of the observation that within the experimental error bars the Q^2-dependence of the forward transverse cross section was satisfactorily

reproduced by the Q^2-dependence of the total virtual-photoproduction cross section. Therefore, $\sigma_{\rm T}(Q^2)$ was parameterized with the overall scale as a free parameter, and the parameterized values then used to subtract $\sigma_{\rm T}$ from the measured unseparated cross sections to obtain $\sigma_{\rm L}$. These $\sigma_{\rm L}$ data at the lowest value of $-t$ were used to determine F_π, assuming that $\sigma_{\rm L}$ is given there by the t-channel one pion-exchange Born term. This was done for all data obtained at CEA and Cornell. The uncertainties in F_π thus obtained and presented in Ref. [12] are statistical ones only, and do not include the contribution from the uncertainty in the value of $\sigma_{\rm T}$ used in the subtraction. Especially at the larger values of Q^2, these are considered to be substantial, as can be seen from Fig. 4 of Ref. [12].

The DESY experiments produced high-quality separated cross sections at $Q^2 = 0.35$ GeV^2, $W = 2.10$ GeV [13] and $Q^2 = 0.70$ GeV^2, $W = 2.19$ GeV [14]. Both of these experiments used the generalized Born Term Model of Gutbrod and Kramer [32] to determine F_π. This BTM incorporates t, s, and u-channel diagrams for the $\gamma_v + p \to \pi^+ + n$ reaction, giving a fair description of the magnitude of the measured unseparated cross sections, but failing to describe $\sigma_{\rm TT}$ and $\sigma_{\rm LT}$. However, Gutbrod and Kramer found that when treating the magnitude of the nucleon form factor $G_E^p(Q^2)$ as a free parameter, a much better description of the then available data was obtained. In addition, they included a factor e^{t/M^2} in order to improve the description of the t dependence of the data. The justification given is that the nucleon is far off its mass-shell, whereas the pion is near to its pole. This generalized BTM gave a good overall description of the DESY data. However, at $Q^2 = 0.70$ GeV^2, nucleon form factors about 50% above their on-mass-shell values were needed. The size of the modification needed at $Q^2 = 0.35$ GeV^2 is not given.

C. Newer Models

More recently, two new models for the $^1{\rm H}(e,e'\pi^+)n$ reaction have become available.

In Refs. [23, 33], Vanderhaeghen, Guidal and Laget (VGL) have presented a Regge model for pion production in which the pole-like propagators of Born term models are replaced with Regge propagators, i.e., the interaction is effectively described by the exchange of a family of particles with the same quantum numbers instead of a single particle. If the same vertices and coupling constants are used, the Regge model and the BTM calculations agree at the pole of the exchanged particle, but away from the pole the Regge model provides a superior description of the available data. For forward pion production, the dominant exchanges are the π and ρ trajectories. These determine the t-dependence of the cross section without the use of a $g_{\pi NN}(t)$ factor. At low values of $-t$, as covered by this work, $\sigma_{\rm L}$ is completely determined by the π trajectory, while $\sigma_{\rm T}$ is also sensitive to the ρ exchange contribution. Since the t-channel π diagram is by itself not gauge invariant, the s-channel (for π^+ production) or u-channel (for π^- production) nucleon exchange diagram was also Reggeized, to ensure gauge invariance of their sum.

The VGL model was first applied to pion photoproduction [33] and later extended to electroproduction [23], with monopole forms for the $\pi\pi\gamma$ and $\rho\pi\gamma$ form factors:

$$F_{\pi,\rho}(Q^2) = [1 + Q^2/\Lambda^2_{\pi,\rho}]^{-1}. \qquad (7)$$

Apart from the $\pi\pi\gamma$ and $\rho\pi\gamma$ form factors, the model is parameter free, as the coupling constants at the vertices (such as $g_{\rho\pi\gamma}$) are well determined by precise studies and analyses in the resonance region. The model gives a good description of the W- and t-dependences of then available π^+ and π^- photoproduction data, including the spin asymmetries, and of the earlier electroproduction data.

The VGL predictions have been compared to our measured cross sections and the ones taken at DESY [13, 14] in Ref. [18]. For the discussion in this paper, the data for $\sigma_{\rm L}$ and $\sigma_{\rm T}$ are reproduced in Fig. 2, together with the results of the model calculations. The VGL cross sections were evaluated at the same $\overline{W}$ and $\overline{Q^2}$ values as the data, resulting in the discontinuities shown. The values of Λ^2_π shown are determined by the fitting of the VGL model to the measured $\sigma_{\rm L}$-values at the five values of t at each Q^2, resulting in values between 0.37 and 0.51 GeV^2. The value of Λ^2_ρ is more poorly known. Calculations with both Λ^2_ρ=0.600 and 1.500 GeV^2 are shown, where the upper value is taken from the application of the VGL model to kaon electroproduction [34].

The model gives an overall good description of our $\sigma_{\rm L}$ data and those of [13, 14], but the description of the t-dependence of the data is worse at Q^2=0.60 and 0.70 GeV^2. The poorer description of the $\sigma_{\rm L}$ data by the VGL model at lower Q^2 and W may be due to contributions from resonances, which are not included explicitly in the Regge model. This is supported by the fact that the discrepancy in the t-dependence of the $\sigma_{\rm L}$ data is strongest at the lowest Q^2 value, at higher Q^2 the resonance form factor supposedly reducing such contributions. The values of $\sigma_{\rm T}$ are severely underestimated, especially at larger Q^2, even when taking a hard $\rho\pi\gamma$ form factor. Since the data at the real-photon point are well described, this suggests that another mechanism, whose contribution increases with Q^2, is at play [35]. Recently the VGL model was extended [36] by including a hard scattering between the virtual photon and a quark, the latter hadronizing in combination with the spectator diquark into a pion plus residual nucleon. With plausible assumptions, a good description of $\sigma_{\rm T}$ was obtained, with no influence on $\sigma_{\rm L}$. Those results support the idea that the discrepancy in the magnitude of $\sigma_{\rm T}$, which increases with Q^2, and the discrepancy in the slope of $\sigma_{\rm L}$ with $-t$, which decreases with Q^2, are not directly related. Strategies for dealing with the latter discrepancy when extracting the pion form factor are discussed in Sec. III.

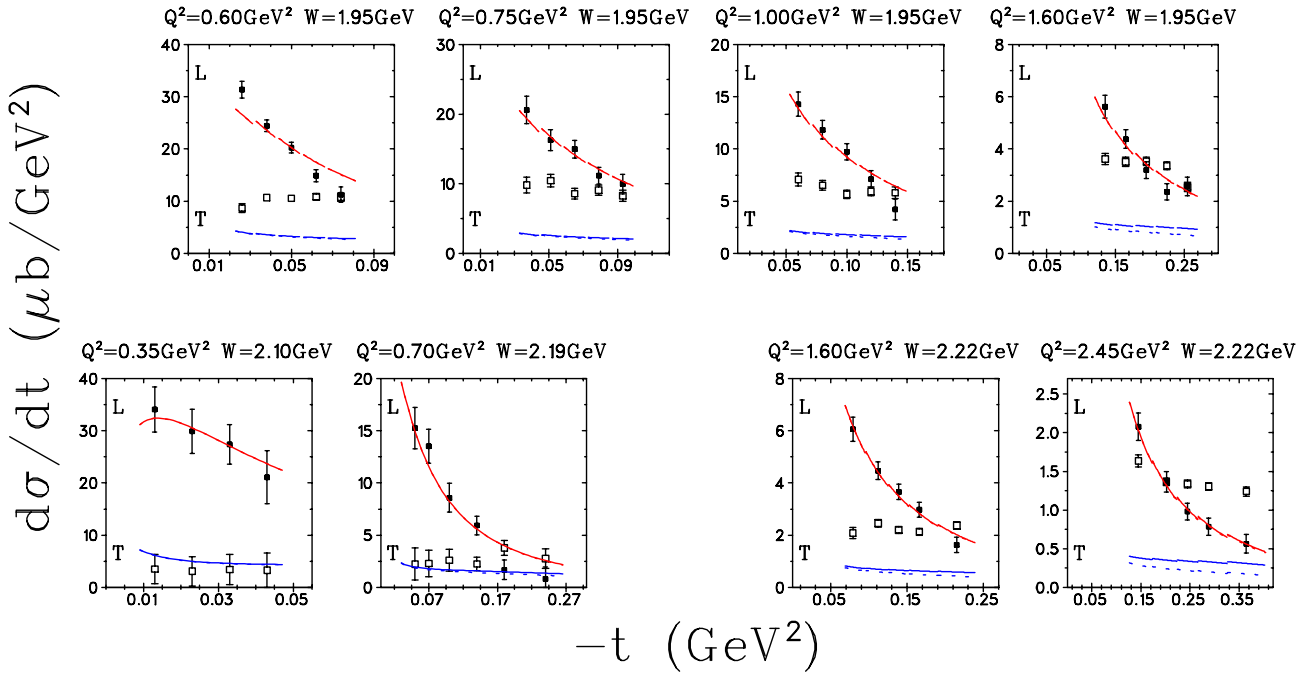

FIG. 2: (Color online) Separated π^+ electroproduction cross sections $\sigma_{\rm L}$ [solid] and $\sigma_{\rm T}$ [open] from JLab and DESY in comparison to the predictions of the VGL Regge model [23]. The error bars of the JLab data represent the combination of statistical and t uncorrelated systematic uncertainties. In addition, there is an overall systematic uncertainty of about 6%, mainly from the t correlated, ϵ uncorrelated systematic uncertainty. The VGL Regge model calculations for Q^2=0.60-1.60 GeV^2, W=1.95 GeV use Λ^2_π=0.394, 0.372, 0.411, 0.455, GeV^2, and those for Q^2=0.35-2.45 GeV^2, $W\sim$ 2.1 GeV use Λ^2_π=0.601, 0.519, 0.513, 0.491 GeV^2. The solid(dashed) curves indicate the Λ^2_ρ=1.500(0.600) GeV^2 value used.

We also considered a modification to the VGL Regge model published by J.M. Laget in 2004 [37]. Laget introduces a t-dependent factor into the pion form factor which is related to the pion saturating Regge trajectory, approaching -1 as $t \to -\infty$. The effect of this modification is to boost $\sigma_{\rm T}$ by 40% for the largest $-t$ spanned by our data (Q^2=2.703 GeV^2, $-t$=0.365 GeV^2), and converging with the unmodified calculation at small $-t$. The effect on $\sigma_{\rm L}$ is under 1% for the largest $-t$ covered by our data, and is negligible at $-t_{min}$.

Another recent development is the effective Lagrangian model of Faessler, Gutsche, Lyubovitskij and Obukhovsky (FGLO, Ref. [38, 39]). This is a modified Born Term Model, in which an effective Lagrangian is used to describe nucleon, pion, ρ and photon degrees of freedom. The (combined) effect of s- and u-channel contributions, which interferes with the pion t-pole, is modeled using a constituent quark model. The authors show that the ρ t-pole contribution is very important in the description of the magnitude of $\sigma_{\rm T}$. When comparing vector and tensor representations of the ρ contribution, the latter was found to give better results. Unlike the VGL model, the $\sigma_{\rm L}$ cross section depends here also on the ρ exchange, because of the interference of the π and tensor ρ exchange contributions. The model contains a few free parameters, such as the renormalization constant of the Kroll-Ruderman contact term used to model the $s(u)$-channel, and t-dependent strong meson-nucleon vertices, which are parameterized in monopole form, as are the electromagnetic form factors. The corresponding parameters were adjusted so as to give overall good agreement with our $\sigma_{\rm L}$ and $\sigma_{\rm T}$ data.

As in case of the VGL model, a detailed comparison of the FGLO model results to the measured data is given in Ref. [18], while the results for $\sigma_{\rm L}$ and $\sigma_{\rm T}$ are also shown in Fig. 3. The values of Λ^2_π used were determined by the fitting of the model to the $\sigma_{\rm L}$ t-bins at each Q^2, while keeping the other parameters fixed at the values assigned by the authors. In some cases, this results in different Λ^2_π values than shown in Ref. [39]. However, it should be kept in mind that the FGLO model $\sigma_{\rm L}$ cross sections also depend on other parameters, which have been adjusted by the authors of the model to give good agreement to our $\sigma_{\rm L}$ and $\sigma_{\rm T}$ data. To the best of our knowledge, the Q^2=0.7 GeV^2 data of Ref. [14] were not taken into account when these parameters were determined.

Generally, the agreement of the FGLO model with the $\sigma_{\rm L}$ data is rather good except for the Q^2=0.60 [Fpi-1] and 0.70 GeV^2 [14] measurements. There is a serious discrepancy in the Q^2- and W-dependence of the $\sigma_{\rm T}$ data. For Q^2 around 0.7 GeV^2, the model agrees fairly well with the data at W = 1.95 GeV, but it over-predicts the Q^2=0.70 GeV^2, W = 2.19 GeV data by a large factor. On the other hand, for Q^2=1.60 GeV^2, the W = 1.95 GeV data are under-predicted by about a factor of two, while those at W = 2.22 GeV are reproduced, and the W = 2.22 GeV data for Q^2=2.45 GeV^2 are under-predicted again by 20-60%. This indicates some problem in the description of the Q^2, W-dependences of the ρ exchange used to describe $\sigma_{\rm T}$. Because of the $\rho - \pi$ interference, the problems with the description of $\sigma_{\rm T}$ also affect the $\sigma_{\rm L}$ calculation. This makes it hard to estimate how reliable the values of F_π would be if extracted from the data using this model.

Q^2 (GeV^2)	W (GeV)	Λ^2_π (GeV^2)	F_π
0.60	1.95	$0.458 \pm 0.031^{+0.255}_{-0.068}$	$0.433 \pm 0.017^{+0.137}_{-0.036}$
0.75	1.95	$0.388 \pm 0.038^{+0.135}_{-0.053}$	$0.341 \pm 0.022^{+0.078}_{-0.031}$
1.00	1.95	$0.454 \pm 0.034^{+0.075}_{-0.040}$	$0.312 \pm 0.016^{+0.035}_{-0.019}$
1.60	1.95	$0.485 \pm 0.038^{+0.035}_{-0.027}$	$0.233 \pm 0.014^{+0.013}_{-0.010}$
0.35	2.10	0.601 ± 0.060	0.632 ± 0.023
0.70	2.19	$0.627 \pm 0.058^{+0.096}_{-0.085}$	$0.473 \pm 0.023^{+0.038}_{-0.034}$
1.60	2.22	$0.513 \pm 0.033^{+0.052}_{-0.022}$	$0.243 \pm 0.012^{+0.019}_{-0.008}$
2.45	2.22	$0.491 \pm 0.035^{+0.045}_{-0.024}$	$0.167 \pm 0.010^{+0.013}_{-0.007}$

TABLE I: Λ^2_π and F_π values from this work, and the reanalyzed data from Refs. [13, 14] using the same method. The first error includes all experimental and analysis uncertainties, and the second error is the 'model uncertainty' as described in the text. The total uncertainty is found by taking their sum, in quadrature. Please note that in some cases the Λ^2_π value listed is different than the value used in Fig. 2.

III. F_π RESULTS

As already discussed, the separated cross sections versus t over some range of Q^2 and W are the actual observables measured by the experiment, and the extraction of the pion form factor from these data is inherently model dependent. Ideally, one would like to have a variety of reliable electroproduction models to choose from, so that the model dependence of the extracted F_π values can be better understood. Since the VGL Regge model is able, without fitted parameters, to provide a good description of both π^+ and π^- photoproduction data, and of $\sigma_{\rm L}$ electroproduction data over a range in W, t, and Q^2, it is our opinion that at the moment only this model has shown itself to be sufficiently reliable to enable its use to extract pion form factor values from the $\sigma_{\rm L}$ data. Therefore, we will use this model to determine our F_π values. Clearly, the F_π values determined are strictly within the context of the VGL Regge model, and other values may result if other, better models become available in the future.

A. W $\approx$ 2.2 GeV Data

As shown in Fig. 2, the VGL model does a good job of describing the t-dependence of the $\sigma_{\rm L}$ cross sections at $W \approx 2.2$ GeV, Q^2 =0.35, 1.60 and 2.45 GeV^2. In these cases, the extraction of the pion form factor from the data is straightforward: the value of Λ^2_π in the model

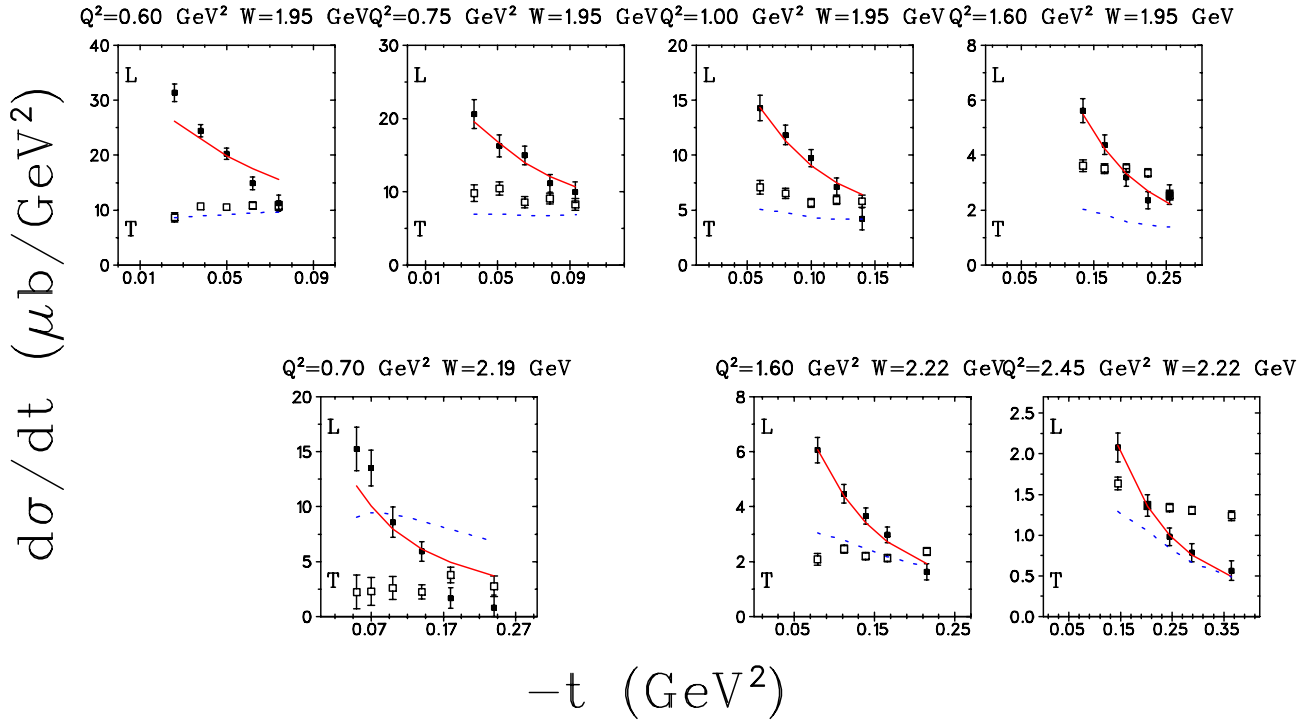

FIG. 3: (Color online) Separated π^+ electroproduction cross sections $\sigma_{\rm L}$ [solid], and $\sigma_{\rm T}$ [open] from this work and DESY [14] in comparison to the FGLO effective Lagrangian model [39]. The data error bars and systematic uncertainties are as in Fig. 2. The solid (dashed) curves denote model calculations for $\sigma_{\rm L}$ ($\sigma_{\rm T}$) with Λ^2_π=0.405, 0.414, 0.503, 0.654, 0.386, 0.608 and 0.636 GeV^2 (from upper left to lower right). The calculations were performed at the same $\overline{W}$ and $\overline{Q}^2$ as the data, with straight lines connecting the calculated values.

is varied until the agreement of the model with the data is optimized. The mean $\overline{Q}^2$ and $\overline{W}$ values of the data for each t-bin are used when evaluating the model. F_π is then calculated from Eqn. 7, using the best-fit Λ_π^2 and the nominal Q^2 values. These are listed in the last two lines of Table I.

The experimental statistical and systematic uncertainties were propagated to the F_π uncertainties as follows. The statistical and t,ϵ-uncorrelated systematic uncertainties[1] were applied to the $\sigma_{\rm L}$ data prior to the fitting of the VGL model to the $\sigma_{\rm L}$ data. This yields the best-fit Λ_π^2 value and its associated fitting uncertainty. The effects of the t-correlated, ϵ-uncorrelated, and the t,ϵ-correlated systematic uncertainties on the fit were determined by investigating the variation in Λ_π^2 values allowed by fitting to the lowest $-t$ bin only. Of these, the ϵ-uncorrelated, t-correlated systematic uncertainty is amplified by $1/\Delta\epsilon$ in the L-T separation, while the t,ϵ-correlated uncertainty is not. The resulting uncertainties are added in quadrature to the fitting error, yielding the first Λ_π^2 uncertainty listed in Table I. This value is also propagated to F_π according to the monopole parameterization, yielding the first F_π uncertainty listed.

In order to check if the extracted value of F_π depends on the t-range used, the VGL model (i.e., the value of Λ_π^2) was fitted separately to each $\sigma_{\rm L}$ point from Fpi-2 and DESY [13, 14], and the corresponding values of F_π determined. In order to remove the natural variation of F_π with the $\overline{Q}^2$ of each bin, the nominal Q^2 values were used in the monopole equation. A plot of the obtained F_π versus t is shown in Fig. 4. Also indicated as the shaded band is the F_π value with the uncertainty that is obtained if one fits to all of the t-bins simultaneously. Except perhaps at Q^2=0.70 GeV^2, the data show no residual t-dependence beyond the statistical fluctuation.

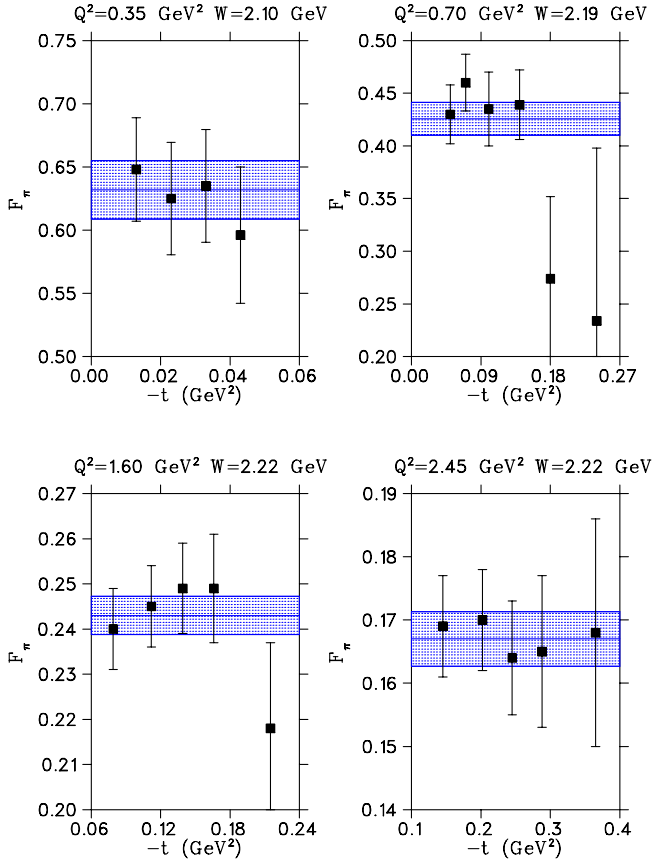

FIG. 4: (Color online) F_π consistency check for the DESY and Fpi-2 data at $W \approx 2.2$ GeV. The solid squares indicate the F_π values that would be obtained if the VGL model was fit to each $\sigma_{\rm L}$ point separately. The shaded band is the F_π value that is obtained if the model is fit to all of the t-bins. The error bars and band reflect the statistical and t-uncorrelated systematic uncertainties only.

B. W = 1.95 GeV Data

As already shown in Sec. II C, the VGL model does not fully describe the t-dependence of our $\sigma_{\rm L}$ data at W = 1.95 GeV. The difficulty, as far as the F_π extraction is concerned, is that there is no theoretical guidance for the assumed interfering background not included in the VGL model, even if one assumes that it is due to resonances. Virtually nothing is known about the L/T character of resonances at W = 1.95 GeV, let alone how they may influence $\sigma_{\rm L}$ through their interference with the π-pole amplitude. Given this lack of theoretical guidance, we are forced to make some assumptions in extracting F_π from these data. Our guiding principle is to minimize these assumptions to the greatest extent possible. The form factor extraction method that we have adopted for these data relies on the single assumption that the contribution of the background is smallest at the kinematic endpoint t_{min}.

Our best estimate of F_π for the W = 1.95 GeV data is determined in the following manner. Using the value of Λ_π^2 as a free parameter, the VGL model was fitted to each t-bin separately, yielding $\Lambda_\pi^2(\overline{Q^2}, \overline{W}, t)$ values as shown in Fig. 5. The values of Λ_π^2 tend to decrease as $-t$ increases, presumably because of an interfering background not included in the VGL model. Since the pole cross section containing F_π increases strongly with decreasing $-t$, we assume that the effect of this background will be smallest at the lowest value of $|t|$ allowed by the experimental kinematics, $|t_{min}|$. Thus, an extrapolation of Λ_π^2 to this physical limit is used to obtain our best estimate of F_π. The value of Λ_π^2 at t_{min} is obtained by a linear fit to the data in Fig. 5. The resulting Λ_π^2 and F_π values for the Fpi-1 data are listed in Table I. The first uncertainty listed includes both the experimental and the linear fit extrapolation uncertainties.

Since Fig. 4 suggests also a dependence (at larger $-t$)

[1] These uncertainties are described in detail in Ref. [18]

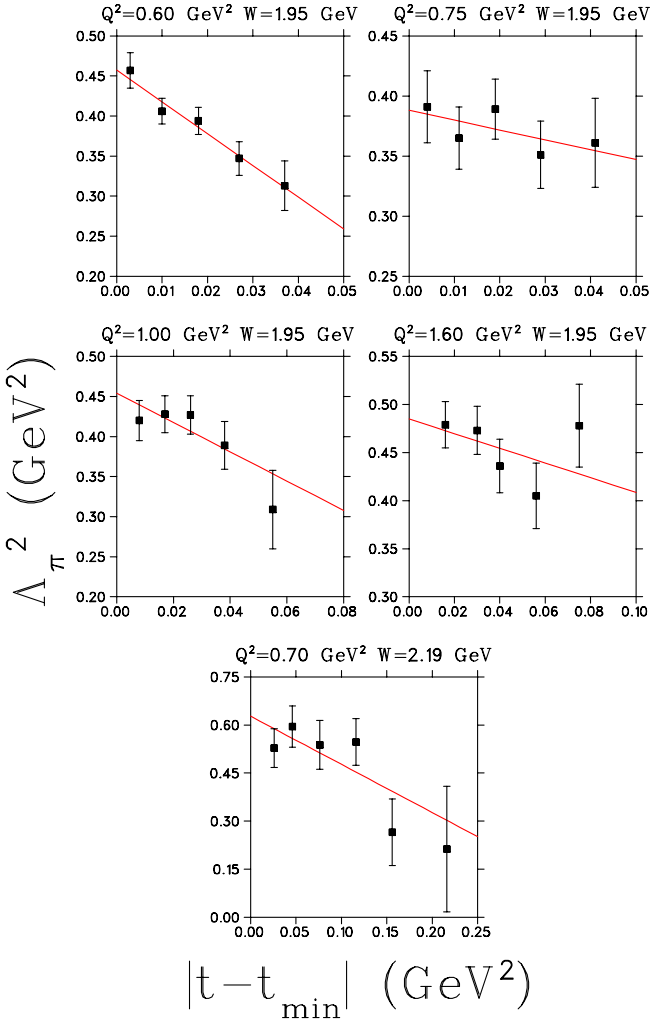

FIG. 5: (Color online) Values of Λ_π^2 determined from the fit of the VGL model to each t-bin, and linear fit to same. The error bars reflect the statistical and t-uncorrelated systematic uncertainties. The additional overall systematic uncertainties, which were applied after the fit, are not shown.

between the VGL calculation and the Q^2=0.70 GeV^2 data of Ref. [14], this F_π extraction method was also applied to those data. The result obtained when extrapolating to t_{min} is listed in Table I. The value of $F_\pi(\Lambda_\pi^2)$ is 11(20)% larger than if the VGL model was simply fit to all data points. Applying the same procedure to our W = 2.22 GeV data, it was found that the resulting values of $F_\pi(\Lambda_\pi^2)$ would be 1(2)% larger, which is statistically insignificant, confirming that the t-dependence of those data is well described by the VGL model.

C. Model Uncertainty Estimate

The fact that we used an additional assumption for the cases where the VGL model does not completely describe the t-dependence of the σ_L data causes an additional uncertainty in the extracted F_π value, which we term 'model uncertainty'. This model uncertainty, which is within the context of the VGL model, should be distinguished from the general model uncertainty discussed in section II, which would result when using different models. In order to make a quantitative estimate of this additional uncertainty, the spread in extracted values of Λ_π^2 (and thus F_π) was investigated by assuming specific forms of the interfering background missing in the VGL model.

An effective upper limit for F_π is obtained by assuming that the background yields a constant, negative, contribution to σ_L. For each value of Q^2, this background and the value of Λ_π^2 were fit together to the data, assuming that the background is constant with t. The fitted contribution of the background was found to drop strongly with increasing Q^2. A second possibility is to assume, besides the VGL amplitude, a t-independent interfering background amplitude, fitting for every Q^2 the magnitude and phase of the latter, together with the value of Λ_π^2. Although the fitting uncertainties are very large, the results suggest an interfering amplitude whose magnitude decreases monotonically with increasing Q^2. In this case, the interference between the background amplitude and the VGL amplitude, which depends on their relative phase, does not necessarily result in a net negative cross section contribution to σ_L.

The estimated model uncertainty is determined from the spread of the Λ_π^2 values and their uncertainties at each Q^2, obtained with these two choices of background. To keep the number of degrees of freedom the same in both cases, the background was fixed to the value giving the best χ^2, and Λ_π^2 and its uncertainty were then determined in a one-parameter fit of the VGL model plus background to the data. Since the statistical uncertainties of the data are already taken into account in the first given uncertainty in Table I, the contribution of the statistical uncertainties of the data were quadratically removed from the Λ_π^2 uncertainties given by the fit. The model uncertainties at each Q^2 are then taken as the range plus corrected fitting uncertainty given by these two methods, relative to the value of Λ_π^2 determined from the extrapolation to t_{min}. This procedure was applied to all data except those of Ref. [13], yielding the model uncertainties listed as the second (asymmetric) uncertainty in Table I. No model uncertainty was calculated for the Q^2=0.35 GeV^2 data from DESY because the t-range spanned by those data (only 0.03 GeV^2) was too small for this procedure to be reliably applied.

For the W = 1.95 GeV data, the model uncertainty in the extracted F_π value drops from about 20% at Q^2=0.60 GeV^2 to about 5% at 1.60 GeV^2. To be consistent, the same procedure was applied to the W = 2.22 GeV data, which yielded model uncertainties of about 5% at both Q^2=1.60 and 2.45 GeV^2. These rapidly dropping uncertainties with increasing Q^2 reflect the smaller discrepancy of the VGL calculation with the t-dependence of the data

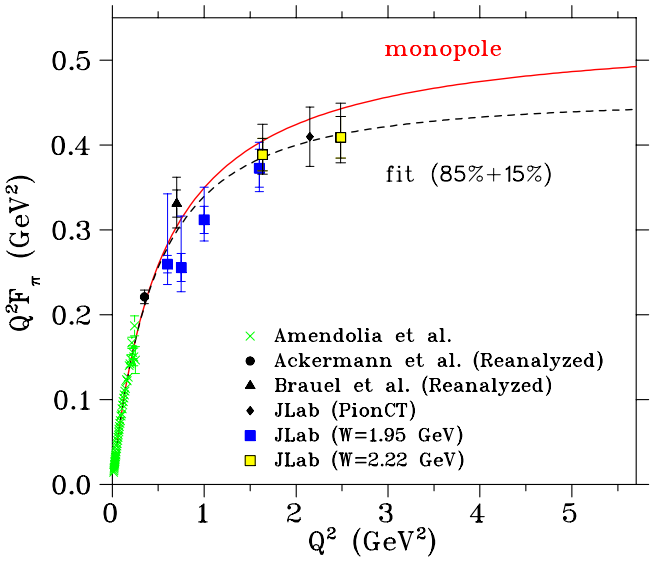

FIG. 6: (Color online) Q^2F_π data from this work, compared to previously published data. The solid Brauel *et al.* [14] point has been reanalyzed as discussed in the text. The outer error bars for the JLab data and the reanalyzed Brauel *et al.* data include all experimental and model uncertainties, added in quadrature, while the inner error bars reflect the experimental uncertainties only. Also shown is the monopole fit by Amendolia *et al.* [9] as well as a 85% monopole+15% dipole fit to our data.

at larger values of Q^2 and W. These findings are at least compatible with the idea that resonance contributions, which presumably have a form factor that drops rapidly with Q^2, are responsible. They also suggest that our F_π extraction methods are robust, when the background contribution is small, as appears to be the case at the higher value of W.

D. Discussion and Comparison with Empirical Fits

The form factors extracted from the Fpi-1 and Fpi-2 data with the use of the VGL model are shown in Fig. 6, along with the reanalyzed Q^2=0.70 GeV^2 data of Ref. [14], the elastic scattering measurements of Ref. [9], and the Q^2=0.35 GeV^2 data of Ref. [13]. The Cornell data of Refs. [10, 11, 12] are not included because, as discussed in section II B, they have large unknown systematic uncertainties. The excellent agreement between the Q^2=1.6 GeV^2 form factor values obtained from our $W = 1.95$, 2.22 GeV data, despite their significantly different t_{min} and W values, indicates that the model uncertainties from the use of the VGL model seem to be under control, at least in this Q^2-range. Also shown is a more recently obtained value at Q^2=2.15 GeV^2 [40], which was also extracted with the use of the VGL model.

The solid line shown in Fig. 6 is the monopole fit obtained by Amendolia *et al.* [9] from their elastic scattering data. This curve is given by

$$F_{mono} = \frac{1}{1 + \frac{r^2_{mono}Q^2}{6\hbar^2c^2}}, \tag{8}$$

where $r^2_{mono} = 0.431$ fm^2 is their best-fit squared pion charge radius. Fig. 6 indicates a systematic departure of the data from the monopole curve above $Q^2 \approx 1.5$ GeV^2. This departure may have implications for theoretical approaches that assume the validity of the monopole parameterization over a wide range of Q^2.

To illustrate the departure from the monopole curve, as well as to provide an empirical fit that describes the data over the measured Q^2 range, we also show in Fig 6 a fit which includes a small dipole component,

$$F_{fit} = 85\%F_{mono} + 15\%F_{dip}, \tag{9}$$

where

$$F_{dip} = \frac{1}{\left(1 + \frac{r^2_{dip}Q^2}{12\hbar^2c^2}\right)^2} \tag{10}$$

, and $r^2_{dip} = 0.411$ fm^2. This dipole parameterization has nearly the same χ^2 for the elastic scattering data as the monopole curve shown [9], but it drops much more rapidly with Q^2. The combined monopole plus dipole fit is consistent with our intermediate Q^2 data, while maintaining the quality of fit to the elastic scattering data. Since a monopole parameterization does not converge to the pQCD asymptotic limit (Eqn. 2), it is expected to fail at some point. Similarly, we should expect this empirical monopole+dipole parameterization to show its limitations when additional high Q^2 data become available [41].

IV. COMPARISON WITH MODEL CALCULATIONS

The pion form factor can be calculated relatively easily in a large number of theoretical approaches which help advance of our knowledge of hadronic structure. In this sense, F_π plays a role similar to that of the positronium atom in QED. Here, we compare our extracted F_π values to a variety of calculations, selected to provide a representative sample of the approaches used.

A. Perturbative QCD

The most firmly grounded approach for the calculation of F_π is that of pQCD. The large Q^2 behavior of the pion form factor has already been given in Eqn. 1. By making use of model-independent dimensional arguments, the infinitely-large Q^2 behavior of the pion's quark wave function (distribution amplitude, or DA) is identified as

$$\phi_\pi(x, Q^2 \to \infty) \to 6f_\pi x(1-x) \tag{11}$$

whose normalization is fixed from the $\pi^+ \rightarrow \mu^+\nu_\mu$ decay constant. Eqn. 2 follows from this expression.

Neither of these equations is expected to describe the pion form factor in the kinematic regime of our data, and so much effort has been expended to extend the calculation of F_π to experimentally accessible Q^2. In this case, the pion DA, $\phi_\pi(x, Q^2)$, must be determined at finite Q^2. Additional effects, such as quark transverse momentum and Sudakov suppression (essentially a suppression of large quark-quark separation configurations in elastic scattering processes) must be taken into account. A number of authors [42, 43, 44, 45, 46] have performed leading-twist next-to-leading order (NLO) analyses of F_π at finite Q^2. The hard contributions to F_π expand as a leading order part of order α_s and an NLO part of order α_s^2.

Bakulev, Passek-Kumericki, Schroers and Stefanis [47] have investigated the dependence of the form of the DA on the form factors, using data from a variety of experiments. These were the $\pi\gamma\gamma$ transition form factor data from CLEO [48] and CELLO [49], as well as our F_π data. Their results are insensitive to the shape of the DA near $x = 1/2$, while its behavior at $x = 0$, 1 is decisive. The resulting hard contribution to the pion form factor is only slightly larger than that calculated with the asymptotic DA in all considered schemes. The result of their study, shown as F_π^{hard} in Fig. 7, is far below our data. The drop

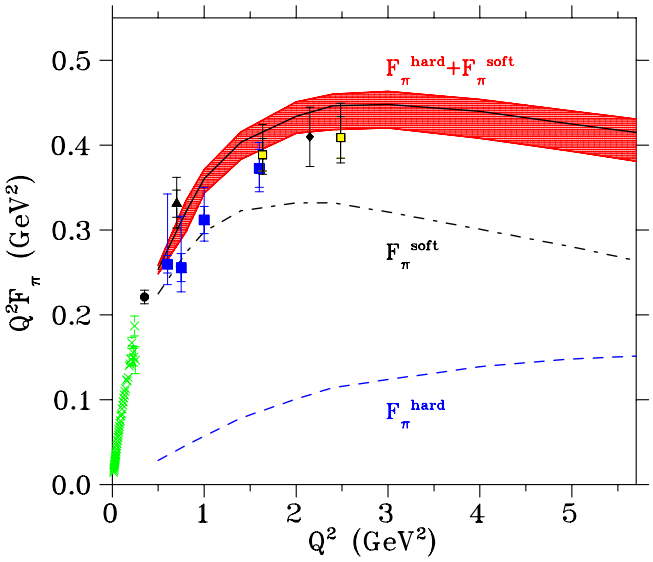

FIG. 7: (Color online) The F_π data of Fig. 6 are compared with a hard LO+NLO contribution by Bakulev, Passek-Kumericki, Schroers and Stefanis [47] based on an analysis of the pion-photon transition form factor data from CLEO [48] and CELLO [49]. A soft component, estimated from a local quark-hadron duality model, is added to bring the calculation into agreement with the experimental data. The band around the sum reflects nonperturbative uncertainties from nonlocal QCD sum rules and renormalization scheme and scale ambiguities at the NLO level.

at low Q^2 is due to their choice of infrared renormalization, which is not necessarily shared by other calculations. To bring the calculation into agreement with the experimental data, a soft component must also be added. The treatment of the soft contribution to the pion DA is model-dependent. The authors estimate this soft contribution using a local quark-hadron duality model. This soft estimate, along with the sum of the hard and soft contributions, are also shown in Fig. 7.

The interplay at intermediate Q^2 between the hard and soft components can be non-trivial, as demonstrated by Braun, Khodjamirian, and Maul [5], using a light-cone sum rule approach. Their results support a pion DA that is close to the asymptotic expression, but they find that strong cancellations between soft terms and hard terms of higher twist lead to the paradoxical conclusion that the nonperturbative effects in the pion form factor can be small, and the soft contributions large, simultaneously. Because of complications such as these, different theoretical viewpoints on whether the higher-twist mechanisms dominate F_π until very large momentum transfer, or not, remain.

B. Lattice QCD

Unlike QCD-based models, in which confinement must be explicitly added, Lattice QCD allows calculation from first principles. However, while lattice QCD is based on the QCD Lagrangian, it involves a number of approximations. Errors are introduced because space and time are crudely discretized on the lattice. This error is controlled by the use of improved lattice QCD actions. To allow a more rapidly converging action, and hence reduce CPU usage, the pion mass used is significantly larger than the physical pion mass. Chiral extrapolation errors are introduced when the lattice results, determined with large pion mass, are extrapolated to physical values. Finally, quenching errors are introduced when disconnected quark loops are neglected.

The first lattice simulations of F_π were done in the 1980's [50, 51, 52]. These pioneering works were primarily a proof of principle of the lattice technique, and were restricted to $Q^2 < 1$ GeV^2. These results are consistent with the low Q^2 experimental data, within the large statistical uncertainties of these pioneering calculations. Spurred by advances in CPU power and lattice techniques, as well as the availability of new experimental data, a number of groups [53, 54, 55, 56, 57, 58, 59, 60, 61] have returned to the calculation of F_π on the lattice. Of these, we compare our data to the recent unquenched simulations of Brommel, *et al.* [60]. They performed simulations for a wide range of pion masses and lattice spacings, so that both the chiral and continuum limits could be studied. However, the lowest pion mass used in the simulations was 400 MeV, so the chiral extrapolation is significant. The authors fitted the Q^2-dependence of each lattice configuration with a monopole form for

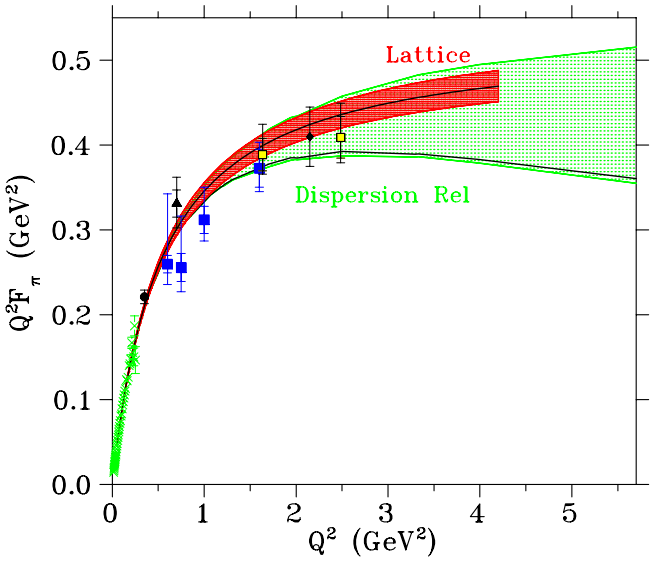

FIG. 8: (Color online) The F_π data of Fig. 6 are compared with the lattice QCD result of Ref. [60] and the dispersion relation result of Ref. [64]. The lattice QCD band denotes the statistical and chiral extrapolation uncertainties in the fit monopole mass to the simulated data. The dispersion relation uncertainty band reflects different assumptions on the distributions of zeroes in the complex s-plane, with the 'no zeroes' curve lying close to the 'minimum F_π' limit.

the pion form factor and determined the corresponding monopole mass. They then extrapolated these masses to the one corresponding to the physical pion mass to obtain a chiral monopole mass value of 0.727 ± 0.016 GeV. The (monopole) form factor calculated with that mass (including its uncertainty) is indicated by the shaded band in Fig. 8, cut off at the highest Q^2 point of the lattice simulation. This result begins to trend away from the $Q^2 > 1.5$ GeV^2 experimental data. It remains to be seen how these results would be affected by our Sec. III D comments on the applicability of the monopole parameterization in this Q^2 range.

C. Dispersion Relation with QCD Constraint

Dispersion relations are based on constraints posed by causality and analyticity, and relate the timelike and spacelike domains of the pion form factor on the complex plane. In principle the technique is exact, but our incomplete knowledge of the scattering amplitudes over the whole complex plane, and in particular the incomplete understanding of the contribution of all of the poles in the timelike region, creates uncertainties. Authors address these uncertainties by imposing additional constraints, such as the role of higher timelike resonances like the ρ''', or chiral perturbation constraints near the spacelike threshold, or that F_π must approach its expected asymptotic value at very large Q^2 [62, 63, 64, 65, 66]. We compare the F_π data to the dispersion relation analysis of B.V. Geshkenbein [64] in Fig. 8. The displayed uncertainty band is obtained by assuming different distributions of zeroes in the complex s-plane. This results in a band that grows with Q^2, with the 'no zeroes' curve lying nearly at the lower end of the band. Our highest Q^2 data lie above the 'no zeroes' curve, but below the 'improved maximum F_π' limit.

D. QCD Sum Rules

The QCD sum rule approach is designed to interpolate between the perturbative and non-perturbative sectors using dispersion relation methods in combination with the operator-product expansion. While the practical implementation of this approach cannot claim to be rigorously derived from QCD, its intuitive value is that it provides a bridge between the low- and high-energy properties of QCD [67]. A number of authors have applied this technique with good success to the pion form factor [5, 6, 68, 69, 70]. In the calculation of Radyushkin [69], QCD sum rules were used to give a local quark-hadron duality estimate of the soft wave function

$$F_\pi^{soft}(Q^2) = 1 - \frac{1 + 6s_0/Q^2}{(1 + 4s_0/Q^2)^{3/2}}, \qquad (12)$$

where the duality interval, s_0, which within the QCD sum rule approach is determined by the magnitude of the quark and gluon condensates, was taken as $4\pi^2 f_\pi 2 \approx 0.7$ GeV^2. This soft calculation, shown in Fig. 9, underestimates the data by about 25%. For the hard contribution, a simple model based on the interpolation between the behavior near $Q^2 = 0$ (related by the Ward identity to the $O(\alpha_s)$ term of the 2-point correlator) and the asymptotic behavior was used

$$F_\pi^{hard}(Q^2) = \frac{\alpha_s}{\pi} \frac{1}{(1 + Q^2/2s_0)}. \qquad (13)$$

The sum, $F_\pi^{soft} + F_\pi^{hard}$, is in excellent agreement with the data.

More recently, Braguta, Lucha and Melikhov [6] have replaced the simple ansatz leading to Eqn. 12 with an expression including explicit corrections up to $O(\alpha_s)$. Since the higher-order corrections needed to apply these results with authority to the intermediate Q^2 region are beyond the capacity of their two-loop calculation, there is a model dependence in their numerical result, which is reflected in the two different curves for $s_0 = 0.65$ GeV^2 and $s_0 = \frac{4\pi^2 f_\pi^2}{1+\alpha_s(Q^2)/\pi}$ shown in Fig. 9.

E. Bethe-Salpeter Equation

The Bethe-Salpeter equation (BSE) is the conventional formalism for the treatment of relativistic bound states.

In this formalism, a meson is described by a covariant wavefunction, which depends on the four momenta of its constituent quarks. Although formally correct, complications arise as the interplay between different configurations, such as q-$\bar{q}$ and q-$\bar{q}$-g, are implicitly buried in the potential and scattering amplitudes used in analyzing hadronic processes, and as a result, these potentials and scattering amplitudes are nearly intractable. The light-front Bethe-Salpeter model is a means to handle this problem by breaking the BSE into separate hard and soft components. A variety of models incorporating a confining potential which dominates at low Q^2, and a QCD-based interaction which dominates at high Q^2, are given in Refs. [71, 72, 73, 74, 75].

Another approach is to use the Dyson-Schwinger equation (DSE) to obtain dressed quark propagators which may be used in the solution of the BSE. The Dyson-Schwinger approach to nonperturbative QCD has many advantages. It is consistent with quark and gluon confinement, it automatically generates dynamical chiral symmetry breaking, and the solution is Poincare invariant. In the work of Maris, Tandy, and Roberts, the meson Bethe-Salpeter amplitudes and quark-photon vertex are obtained as solutions of the homogeneous and inhomogeneous BSE, and the dressed quark propagators are obtained from the quark DSE. The model parameters are fixed by requiring f_π and m_π to be in good agreement with the data [76] and then r_π and F_π are predicted with no further adjustment of parameters [77, 78]. Their calculation is shown in Fig. 9. It is in excellent agreement with our data up to Q^2=1.60 GeV^2. To extend the validity of the model to higher Q^2, a more complete description that takes meson loop corrections into account self-consistently is required [78].

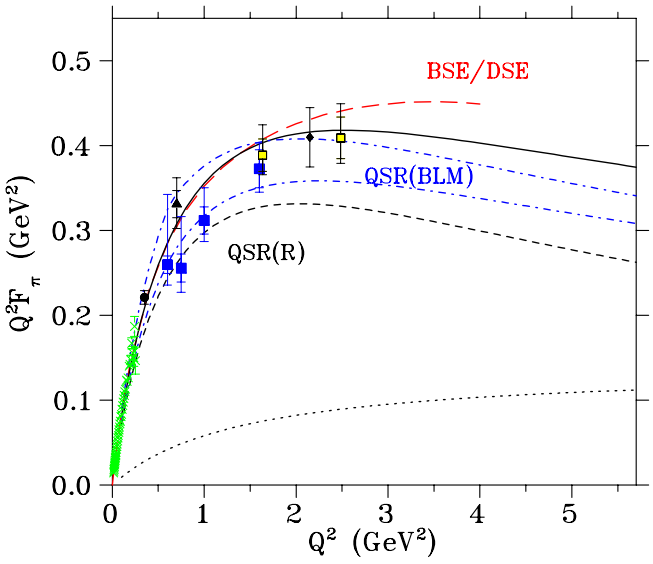

FIG. 9: (Color online) The F_π data of Fig. 6 are compared with the QCD Sum Rules calculations of Refs. [6, 69] and the Bethe-Salpeter equation model utilizing dressed quark propagators via the Dyson-Schwinger equation of Ref. [78] [long dashed]. For the calculation of Ref. [69], three curves are shown: [dotted] F_π^{hard}, [short-dashed] F_π^{soft}, and [solid] the sum $F_\pi^{soft} + F_\pi^{hard}$. For the calculation of Ref. [6], two dot-dashed curves are shown: [lower] $s_0 = \frac{4\pi^2 f_\pi^2}{1+\alpha_s(Q^2)/\pi}$, [upper] $s_0 = 0.65$ GeV^2.

F. Local Quark-Hadron Duality

Quark-hadron duality relations link the hadronic structure information contained in exclusive form factors and inclusive structure functions by making strong assumptions of locality [79]. While local quark-hadron duality is an expected consequence of QCD at asymptotically large momenta, it is not at all clear how well it could work at finite Q^2 [80]. And if it does, it may be due to accidental cancellations of higher twist effects. Nevertheless, it is worthwhile to compare predictions based on quark-hadron duality with the measured data, especially since duality is expected to work better at higher Q^2, in contrast to many other approaches.

The approximate relationship between the pion elastic form factor and the pion structure function $F_2^\pi = \nu W_2^\pi$ was found by Moffat and Snell [81],

$$[F_\pi(Q^2)]^2 \approx \int_1^{\omega_{max}} F_2^\pi(\omega) d\omega, \qquad (14)$$

where $\omega = 1/x$, and the upper limit of integration is chosen to select the elastic contribution to the inclusive structure function. In applying this formula use is made of the Drell-Yan-West [82, 83] relation, which is based on a field-theoretic parton model that predates QCD. It predicts that if the asymptotic behavior of a form factor is $(1/Q^2)^n$, the corresponding structure function should behave as $(1-x)^{2n-1}$ as $x \to 1$. This leads to the prediction $F_2^\pi(x \to 1) \sim (1-x)$.

The existence of Drell-Yan F_2^π data allows a quantitative test of Eqn. 14 using only phenomenological input. Calculations [84, 85] based on the leading-order analysis of F_2^π data by Ref. [86], and the next-to-leading order analysis of Ref. [87], are shown in Fig. 10. In both cases, the magnitude of the F_π prediction is dependent on the value chosen for the inelastic cutoff ω_{max} (and corresponding W_{max}) in Eqn. 14. Local duality is expected not to work at lower Q^2. This is reflected in the poor description of the $Q^2 < 1$ GeV^2 form factor data. However, above $Q^2 > 2$ GeV^2, the next-to-leading order analysis is consistent with our data.

G. Constituent-Quark Model

There are many F_π calculations using a variety of constituent-quark models [88, 89, 90, 91, 92, 93, 94, 95, 96, 97, 98]. The differences in approach typically involve

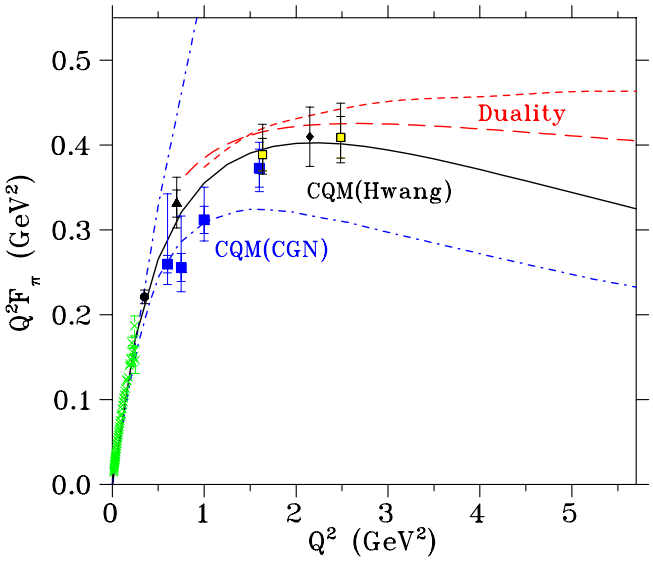

FIG. 10: (Color online) The F_π data of Fig. 6 are compared with the local quark-hadron duality analysis of W. Melnitchouk [84, 85], and the constituent quark model calculations of Refs. [92, 93]. For the duality calculation, two curves are shown: [short-dashed] leading-order analysis of Ref. [84], [long-dashed] next-to-leading order analysis of Ref. [85]. For the quark model calculations by Cardarelli *et al.* [92], two curves are shown: [upper dot-dashed] point-like quarks, [lower dot-dashed] quarks with a monopole form factor.

differences in the treatment of the quark wave functions, or the inclusion of relativistic effects. Fig. 10 shows the result of calculations by Cardarelli *et al.* [92] and by Hwang [93]. Both are relativistic quark models on the light front. Ref. [92] uses the effective $q\bar{q}$ Hamlitonian of [99], which contains a one-gluon-exchange term and a linear confining term, and which describes a large set of meson spectroscopic data. Use of this interaction results in large high-momentum components, and F_π is strongly overpredicted (upper dot-dashed curve in Fig. 10). This can be cured in a way that is consistent with the notion of a constituent quark, by assuming a form factor for the latter. Taking a monopole form for the latter and adjusting the mass parameter so that the measured pion charge radius is reproduced, results in the lower dot-dashed curve shown.

The model of Ref. [93] allows a consistent and fully relativistic treatment of quark spins and center-of-mass motion to be carried out. A power-law wave function is used, whose parameters are determined from experimental data on the charged pion decay constant, the neutral pion two-photon decay width, and the charged pion electromagnetic radius. The charge and transition form factors of the charged pion and the branching ratios of all observed decay modes of the neutral pion are then predicted. The calculation is in very good agreement with our F_π data.

Li and Riska [100] asked if the empirical F_π data exclude the presence of a significant sea-quark configuration in the charged pion. They performed a constituent quark model calculation which was extended to include explicit sea-quark components in the pion wave function. They found that these sea-quark contributions grew with increasing Q^2, because they allowed the momentum transfer to be shared by a greater number of constituents, and so were less-suppressed at high Q^2 than configurations which involved only a $\bar{q}q$ pair. Although their analysis was model-dependent, they found that our data allowed an approximate $20 \pm 20\%$ sea-quark component, with the data point at Q^2=2.45 GeV^2 providing the greatest constraint.

H. Holographic QCD

A recent theoretical development is the AdS/CFT correspondence [101] between weakly-coupled string states defined on a 5-dimensional anti-de Sitter space-time (AdS_5) and a strongly-coupled conformal field theory (CFT) in physical space-time. The goal of holographic QCD models is to find a weakly-coupled theory for which the dual strongly-coupled theory is as close to QCD as possible, and so allow analytic solutions of hadronic properties in the non-perturbative regime to be performed. In these models, confinement is simulated by imposing boundary conditions on the extra fifth dimension z [102]. In the "hard-wall" variant, confinement is modeled by a hard cutoff at a finite value $z = z_0 = 1/\Lambda_{QCD}$. This has the advantage of simplicity but produces the unphysical Regge trajectory $M_n^2 \sim n^2$. The "soft-wall" variant replaces the hard-wall boundary with an oscillator-type potential, and produces the more phenomenologically realistic Regge behavior $M_n^2 \sim n$.

Several authors have applied holographic models to the pion form factor [103, 104, 105, 107]. Complications arise when one introduces spontaneous and explicit chiral symmetry breaking effects into the soft-wall holographic QCD model. Refs. [104, 105] take different approaches to this problem. Grigoryan and Radyushkin [105] consider only the hard-wall variant, and then estimate a soft-wall correction from their previous vector meson study [106]. They conclude that a full analytic calculation would likely follow the F_π data only in the $Q^2 < 1$ GeV^2 region, while overshooting it above $Q^2 \sim 2$ GeV^2. The calculations by Kwee and Lebed [104, 107] are numerical. Both the hard-wall and the soft-wall calculations predict charge radii that are too small, especially for the soft-wall case (see Fig. 11). By allowing the parameters of the soft-wall model (originally fixed by m_ρ, m_π, and f_π) to vary, they find it is possible to describe F_π at either high Q^2 or low Q^2, but not both. Issues in ongoing discussions [105, 107] on the AdS/CFT approach include the applicability of this model to the larger Q^2 region where partonic degrees of freedom become appreciable, and the treatment of chiral symmetry breaking.

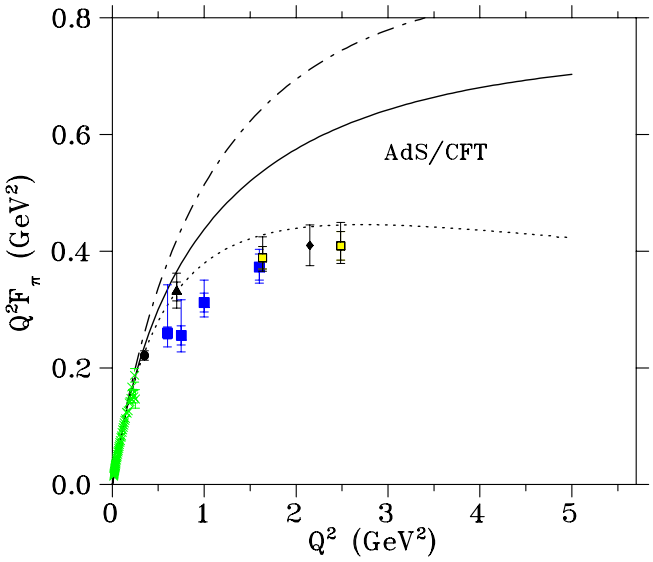

FIG. 11: (Color online) The F_π data of Fig. 6 compared with the holographic QCD model calculations by H.J. Kwee and R.F. Lebed [104]. The curves are: [solid] "hard-wall" and [dot-dash] "soft-wall", both with parameters fit to m_π, m_ρ and f_π, and [dash] "soft-wall" with $\sigma = 262$ MeV to improve the fit to F_π at higher Q^2 but destroying the agreement with the other observables.

V. SUMMARY AND OUTLOOK

Values for the charged pion form factor, $F_\pi(Q^2)$, have been extracted for Q^2=0.60-2.45 GeV^2 from the longitudinal cross sections $\sigma_{\rm L}(t)$ for the ^{1}H$(e,e'\pi^+)n$ reaction recently measured at JLab. F_π values were also extracted from older experimental data acquired at DESY. The Cornell data are not included in this analysis because these $\sigma_{\rm L}$ were not obtained in a true L/T-separation, but instead by subtracting a certain assumption for $\sigma_{\rm T}$. In addition, the higher Q^2 data have excessively large values of $-t_{min}$.

The form factor extraction requires the use of a model incorporating both the π^+ production mechanism as well as the effect of the nucleon. Several approaches to extract F_π from the data, including the Chew-Low extrapolation method, various types of Born Term Models, and newer models utilizing Regge trajectories and effective Lagrangians, were reviewed. By using specially generated test data, it was found that extrapolating to the pole at $t = m_\pi^2$, as is done in the Chew-Low method, cannot be used in practice, because there is no way to determine the order of the polynomial to use for the extrapolation, and because even small uncertainties in the measured cross sections lead to a large uncertainty in F_π.

From the models available for determining F_π from the measured values of $\sigma_{\rm L}$, the VGL Regge model [23] was chosen, since it contains no ad hoc parameters, and its validity has been well established over a wide kinematic range in t and W for both electroproduction and photoproduction data. The VGL model gives a rather good description of both the t and the W dependence of the JLab data at values of $Q^2>$ 1 GeV^2, but especially at Q^2 = 0.60 GeV^2 the fall-off of the data with $-t$ is steeper than that of the model. In the cases where the VGL model described well the t-dependence of the $\sigma_{\rm L}$ data, the value of F_π was determined by fitting the model to the data. Otherwise, the value of F_π was determined by extrapolating the fit of the model to $t = t_{min}$. An additional 'model uncertainty' has been estimated by using two different assumptions for an interfering background that could be responsible for this discrepancy between the data and VGL model. The fact that the discrepancy, and hence the model uncertainty, is very small at higher values of Q^2 and W suggests that effects from nucleon resonances play a role in the data at lower Q^2 and W.

It is stressed that the cross sections are the actual observables measured by the experiment, and that the extracted values of F_π are inherently dependent on the model used to extract them. The development of additional models for the ^{1}H$(e,e'\pi^+)n$ reaction would allow further exploration of the model dependence of the extraction of F_π from the same cross section data. On the experimental front, proposed measurements [41] after the completion of the JLab upgrade are expected to better establish the validity of any used model by investigating, for example, the W-dependence of the results.

The results for F_π, extracted from our data and from the DESY data with the use of the VGL model, are presented together with their experimental and model uncertainties. Above $Q^2 \approx 1.5$ GeV^2, these data are systematically below the monopole parameterization based on the empirical pion charge radius. The data are also compared to a selection of calculations, including those based on pQCD, Lattice QCD, Dispersion Relations, QCD Sum Rules, Bethe-Salpeter Equation, Local Quark-Hadron Duality, Constituent-Quark Model, and Holographic QCD. There has been tremendous progress in the theory of hadronic structure physics in the past decade, as evident by the many new approaches under development. However at present, the intermediate Q^2 regime remains a significant challenge. Several different approaches concur that up to at least Q^2=2.5 GeV^2, the F_π data are far above the estimated 'hard' (perturbative) contribution, and that 'soft' (non-perturbative) contributions likely dominate in this region. Data expected to be taken [41] after the completion of the JLab upgrade, up to at least Q^2 = 6.0 GeV^2, are expected to indicate whether the higher-twist mechanisms dominate F_π until very large momentum transfer, or not.

VI. ACKNOWLEDGMENTS

The authors thank Drs. Guidal, Laget, and Vanderhaeghen for stimulating discussions and for modifying their computer program for our needs. We also thank Dr. Obukhovsky for supplying the result of their model calcu-

lations and for many informative discussions. This work is supported by DOE and NSF (USA), NSERC (Canada), FOM (Netherlands), NATO, and KOSEF (South Korea).

[1] G.P. Lepage, S.J. Brodsky, Phys. Lett. **87B** (1979) 359.
[2] G.R.Farrar, D.R. Jackson, Phys. Rev. Lett. **43** (1979) 246.
[3] O. Dumbrajs, R. Koch, H. Pilkuhn, G.C. Oades, H. Behrens *et al.*, Nucl. Phys. **B 216** (1983) 277.
[4] N. Isgur and C.H. Llewellyn Smith, Phys. Rev. Lett. **52**, 1080 (1984), Phys. Lett. **B217**, 535 (1989), and Nucl. Phys. **B317** 526 (1989).
[5] V.M. Braun, A. Khodjamirian, M. Maul, Phys. Rev. D **61** (2000) 073004.
[6] V. Braguta, W. Lucha, D. Melikhov, Phys. Lett. **661** (2008) 354.
[7] T.K. Pedla *et al.*, Phys. Rev. Lett. **95** (2005) 261803.
[8] E.B. Dally *et al.*, Phys. Rev. Lett. **48** (1982) 375. E.B. Dally *et al.*, Phys. Rev. D **24** (1981) 1718.
[9] S.R. Amendolia *et al.*, Nucl. Phys. **B277** (1986) 168. S.R. Amendolia *et al.*, Phys. Lett. **146B** (1984) 116.
[10] C.J. Bebek *et al.*, Phys. Rev. D **13** (1976) 25.
[11] C.J. Bebek *et al.*, Phys. Rev. Lett. **37** (1976) 1326.
[12] C.J. Bebek *et al.*, Phys. Rev. D **17** (1978) 1693.
[13] H. Ackermann *et al.*, Nucl. Phys. **B137** (1978) 294.
[14] P. Brauel *et al.*, Z. Phys. **C3** (1979) 101.
[15] J. Volmer *et al.*, Phys. Rev. Lett. **86** (2001) 1713.
[16] V. Tadevosyan *et al.*, Phys. Rev. C **75** (2007) 055205.
[17] T. Horn *et al.*, Phys. Rev. Lett. **97** (2006) 192001.
[18] H.P. Blok *et al.*, Phys. Rev. C THE PRECEDING PAPER IN THIS VOLUME.
[19] T. de Forest, Jr, Ann. Phys. (NY) **45** (1967) 365; J.D. Sullivan, Phys. Lett. **33B** (1970) 179.
[20] C.E. Carlson, J. Milana, Phys. Rev. Lett. **65** (1990) 1717.
[21] W.R. Frazer, Phys. Rev. **115** (1959) 1763.
[22] G.F. Chew, F.E. Low, Phys. Rev. **113** (1959) 1640.
[23] M. Vanderhaeghen, M. Guidal, J.-M. Laget, Phys. Rev. C **57** (1998) 1454.
[24] R.C. Devenish, D.H. Lyth, Phys. Rev. D **5** (1972) 47; Phys.Rev.D **6** (1972) 2067.
[25] A. Actor, J.G. Korner, I. Bender, Il Nuovo Cimento **24A** (1974) 369.
[26] L.N. Hand, Phys. Rev. **129** (1963) 1834.
[27] M. Vanderhaeghen, private communication, 2007.
[28] R. Koch, E. Pietarinen, Nucl. Phys. **A 336** (1980) 331.
[29] T. Meissner, Phys. Rev. C **52** (1995) 3386.
[30] C.N. Brown *et al.* Phys. Rev. D **8** (1973) 92.
[31] F.A. Berends, Phys. Rev. D **1** (1970) 2590.
[32] F. Gutbrod, G. Kramer, Nucl. Phys. **B 49** (1972) 461.
[33] M. Guidal J.-M. Laget, M. Vanderhaeghen, Phys. Lett. **B 400** (1997) 6; Nucl. Phys. **A627** (1997) 645.
[34] M. Guidal J.-M. Laget, M. Vanderhaeghen, Phys. Rev. C **61** (2000) 025204.
[35] J.-M. Laget, private communication, 2006.
[36] M.M. Kaskulov, K. Gallmeister, U. Mosel, arXiv:0804.1834 [hep-ph].
[37] J.M. Laget, Phys. Rev. D **70** (2004) 054023.
[38] I.T. Obukhovsky, D. Fedorov, A. Faessler, Th. GUtsche, V.E. Lyubovitskij, Phys. Lett. **B634** (2006) 220.
[39] A. Faessler, T. Gutsche, V.E. Lyubovitskij, I.T. Obukhovsky, Phys. Rev. C **76** (2007) 025213.
[40] T. Horn *et al.*, arXiv:0707.1794 [nucl-ex].
[41] G.M. Huber, D. Gaskell, JLab proposal E12-06-101, "Measurement of the charged pion form factor to high Q^2."
[42] B. Melic, B. Nizic, K. Passek, Phys. Rev. D **60** (1999) 074004.
[43] N.G. Stefanis, W. Schroers, H.-Ch. Kim, Phys. Lett. **B 449** (1999) 299.
[44] N.G. Stefanis, W. Schroers, H.-Ch. Kim, Eur. Phys. J. C **18** (2000) 137.
[45] M.B. Gay Ducati, W.K. Sauter, Phys. Rev. D **67** (2003) 014014.
[46] T. Huang, X.-G. Xu, Phys. Rev. D **70** (2004) 093013.
[47] A.P. Bakulev, K. Passek-Kumericki, W. Schroers, N.G. Stefanis, Phys. Rev. D **70** (2004) 033014, and erratum Phys. Rev. D **70** (2004)079906.
[48] J. Gronberg *et al.*, Phys. Rev. D **57** (1998) 33.
[49] H.J. Behrend *et al.*, Z. Phys. **C49** (1991) 401.
[50] R.M. Woloshyn, Phys. Rev. D **34** (1986) 605.
[51] G. Martinelli, C.T. Sachradajda, Nucl. Phys. **B306** (1988) 865.
[52] T. Draper, R.M. Woloshyn, W. Wilcox, K.-F. Liu, Nucl. Phys. **B318** (1989) 319.
[53] J. van der Heide, M. Lutterot, J.H. Koch, E. Laermann, Phys. Lett. **B 566** (2003) 131.
[54] Y. Nemoto, Nucl. Phys. (Proc. Suppl.) **B 129** (2004) 299.
[55] J. van der Heide, J.H. Koch, E. Laermann, Phys. Rev. D **69** (2004) 094511.
[56] A.M. Abdel-Rehim, R. Lewis, Phys. Rev. D **71** (2005) 014503.
[57] F.D.R. Bonnet, R.G. Edwards, G.T. Fleming, R. Lewis, D.G. Richards, Phys. Rev. D **72** (2005) 054506.
[58] P.A. Boyle, J.M. Flynn, A. Juttner, C.T. Sachrajda, J.M. Zanotti, Jour. High Energy Phys. **0705** (2007) 016.
[59] C. Alexandrou, G. Koutsou, H. Neff, PoS LAT2006 (2006) 113.
[60] D. Brommel *et al.,* Eur. Phys. J. **C 51** (2007) 335.
[61] S. Simula, arXiv:0710.0097 [hep-lat].
[62] J.F. Donoghue, E.S. Na, Phys. Rev. D **56** (1997) 7073.
[63] W.W. Buck, R.F. Lebed, Phys. Rev. D **58** (1998) 056001.
[64] B.V. Geshkenbein, Phys. Rev. D **61** (2000) 033009.
[65] K. Watanabe, H. Ishikawa, M. Nakagawa, hep-ph/0111168.
[66] D. Melikhov, O. Nachtmann, V. Nikonov, T. Paulus, Eur. Phys. J. C **34** (2004) 345.
[67] A.W. Thomas, W. Weise, "The Structure of the Nucleon", Wiley-VCH, 2001.
[68] V.A. Nesterenko, A.V. Radyushkin, Phys. Lett. **B 115** (1982) 410.
[69] A.V. Radyushkin, Nucl. Phys. **A 532** (1991) 141c.
[70] H. Forkel, M. Nielsen, Phys. Lett. **B 345** (1995) 55.
[71] C.R. Munz, J. Resag, B.C. Metsch, H.R. Petry, Phys. Rev. C **52** (1995) 2110.
[72] J.P.B.C. de Melo, T. Frederico, E. Pace, G. Salme, Nucl.

Phys. **A 707** (2002) 399.
[73] J.P.B.C. de Melo, T. Frederico, E. Pace, G. Salme, Phys. Rev. D **73** (2006) 074013.
[74] A. Szczurek, N.N. Nikolaev, J. Speth, Phys. Rev. C **66** (2002) 055206.
[75] L.S. Kisslinger, H.-M. Choi, C.-R. Ji, Phys. Rev. D **63** (2001) 113005.
[76] P. Maris, C.D. Roberts, Phys. Rev. C **58** (1998) 3659.
[77] P. Maris, P.C. Tandy, Phys. Rev. C **61** (2000) 045202.
[78] P. Maris, P.C. Tandy, Phys. Rev. C **62** (2000) 055204.
[79] W. Melnitchouk, R. Ent, C. Keppel, Phys. Rep. **406** (2005) 127.
[80] N. Isgur, S. Jeschonnek, W. Melnitchouk, J.W. Van Orden, Phys. Rev. D **64** (2001) 054005; S. Jeschonnek, J.W. Van Orden, Phys. Rev. D **65** (2002) 094038.
[81] J.W. Moffat, V.G. Snell, Phys. Rev. D **4** (1971) 1452.
[82] S.D. Drell, T.-M. Yan, Phys. Rev. Lett. **24** (1970) 181.
[83] G.B. West, Phys. Rev. Lett. **24** (1970) 1206; Phys. Rev. D **14** (1976) 732.
[84] W. Melnitchouk, Eur. Phys. J. A **17** (2003) 223.
[85] W. Melnitchouk, private communication, 2006.
[86] J.S. Conway *et al.*, Phys. Rev. D **39** (1989) 92.
[87] K. Wijesooriya, P.E. Reimer, R.J. Holt, Phys. Rev. C **72** (2005) 065203.
[88] V. Anisovich, D. Melikhov, V. Nikonov, Phys. Rev. D **52** (1995) 5295.
[89] F. Cardarelli, E. Pace, G. Salme, S. Simula, Phys. Lett. **B 357** (1995) 267.
[90] T.W. Allen, W.H. Klink, Phys. Rev. C **58** (1998) 3670.
[91] H.-M. Choi, C.-R. Ji, Phys. Rev. D **59** (1999) 074015.
[92] F. Cardarelli *et al.*, Phys. Lett. **B 332** (1994) 1.
F. Cardarelli *et al.*, Phys. Rev. D **53** (1996) 6682.
[93] C.-W. Hwang, Phys. Rev. D **64** (2001) 034011.
[94] A.F. Krutov, V.E. Troitsky, Eur. Phys. J. C **20** (2001) 71.
[95] A. Amghar, B. Desplanques, L. Theussl, Phys. Lett. **B 574** (2003) 201.
[96] A.F. Krutov, V.E. Troitsky, Phys. Rev. C **65** (2002) 045501.
[97] E. Sengbusch, W.N. Polyzou, Phys. Rev. C **70** (2004) 058201.
[98] F. Coester, W.N. Polyzou, arXiv:nucl-th/0405082.
F. Coester, W.N. Polyzou, Phys. Rev. C **71** (2005) 028202.
[99] S. Godfrey, N. Isgur, Phys. Rev. D **32** (1985) 189.
[100] Q.B. Li, D.O. Riska, Phys. Rev. C **77** (2008) 045207.
[101] J.M. Maldacena, Adv. Theor. Math. Phys. **2** (1998) 231.
[102] J. Polchinski, M.J. Strassler, Phys. Rev. Lett. **88** (2002) 031601.
[103] S.J. Brodsky, G.F. de Teramond, Phys. Rev. D **77** (2008) 056007.
[104] H.J. Kwee, R.F. Lebed, Jour. High Energy Phys. **0801** (2008) 027.
[105] H.R. Grigoryan, A.V. Radyushkin, Phys. Rev. D **76** (2007) 115007.
[106] H.R. Grigoryan, A.V. Radyushkin, Phys. Rev. D **76** (2007) 095007.
[107] H.J. Kwee, R.F. Lebed, arXiv:0712.1811 [hep-ph].